Wave Inversion Technology, Report No. 4, pages 49-62

Macro-Velocity Model Inversion from CRS Attributes: The Hubral and Krey algorithm revisited

Ricardo Biloti, Lúcio T. Santos, and Martin Tygel[1]

keywords: *Macro-Velocity Inversion, Common Reflection Surface Method*

ABSTRACT

In conventional processing, the classical algorithm of Hubral and Krey is routinely applied to extract an initial macrovelocity model that consists of a stack of homogeneous layers bounded by curved interfaces. Input for the algorithm are identified primary reflections together with NMO velocities derived from a previous velocity analysis conducted on CMP data. This work presents a modified version of the Hubral and Krey algorithm that is adapted to advantegeously use previously obtained CRS attributes as its input. Some simple synthetic examples are provided to illustrate and explain the implementation of the method.

INTRODUCTION

The CRS method (Birgin et al., 1999) is a recent technique that is becoming an alternative to the conventional seismic process, presenting promising results concerning the generation of simulated zero-offset sections. The CRS parameters give, in addition to a better stacking, more information. In fact, this information can be applied to produce a more reliable velocity model that can be used for further imaging purposes such as depth migration.

This is what our work intends to do. What we will show on this article is that, once we have already made an effort to estimate the CRS parameters to construct a clean simulated zero-offset section, we shall immediately be in the position of inverting a macro-velocity model.

Hyperbolic Traveltime and CRS parameters. The hyperbolic traveltime expression relates the traveltime of two rays. One of them is taken as a reference ray and is called central ray. When this central ray is taken as a normal ray at X_0 (see Figure 1),

[1]**email:** {biloti,lucio,tygel}@ime.unicamp.br

the formula becomes

$$T^2(x_m, h) = \left(t_0 + \frac{2x_m \sin\beta_0}{v_0}\right)^2 + \frac{2t_0 \cos^2\beta_0}{v_0}\,(K_N\, x_m^2 + K_{NIP}\, h^2)\,,$$

with

$$x_m = (x_G + x_S)/2 - x_0 \quad \text{and} \quad h = (x_G - x_S)/2\,,$$

where x_S and x_G are the horizontal coordinate of the source and receiver pair (S, G) near X_0, t_0 is the zero-offset traveltime and β_0 is the angle of emergence at the zero-offset ray with respect to the surface normal at the central point X_0. The quantities K_N and K_{NIP} are the wavefront curvatures of the N-wave and the NIP-wave (Hubral, 1983), respectively, measured at the central point X_0. The traveltime formula above is on the kernel of the CRS method. Therefore, those three parameters, β_0, K_N and K_{NIP} are called CRS parameters.

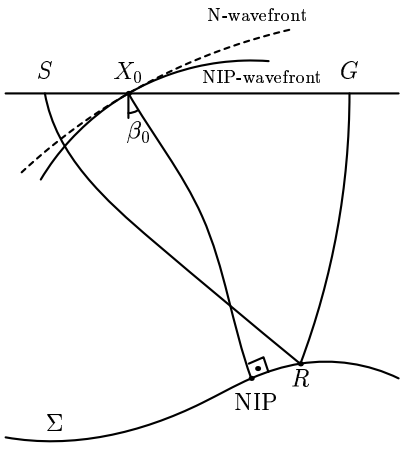

Figure 1: CRS Parameters for a normal central ray X_0 NIP X_0: the emergence angle β_0 and the NIP- and N-wavefront curvatures. Σ is the reflector, X_0 is the central point coordinate, and S and G are the source and receiver positions for a paraxial ray, reflecting at R.

THE HUBRAL AND KREY ALGORITHM

Our inversion method is based on the well established algorithm proposed in Hubral and Krey, 1980. The velocity model to be inverted from the data is assumed to consist of a stack of homogeneous layers bounded by smoothly curved interfaces. The unknowns are the velocity in each layer and the shape of each interface. These unknowns are iteratively obtained from top to bottom by means of a layer stripping process.

The main idea of the algorithm is to backpropagate the NIP-wave down to the NIP located at the bottom interface of the layer to be determined (see Figure 2). This means that the velocities and the reflectors above the layer under consideration have already been determined. Since the NIP-wave is due to a point source at the NIP, the backpropagation through this last layer gives us a focusing condition for the unknown layer velocity.

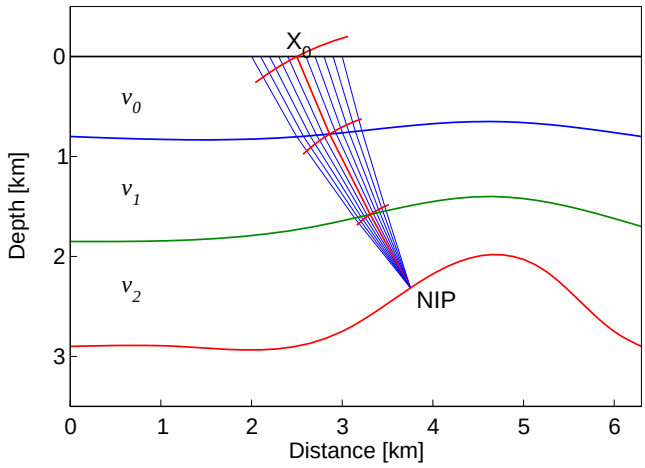

Figure 2: NIP-wavefront associated to the central zero-offset ray X_0 NIP X_0, in red.

To well describe the wavefront curvature along a ray path that propagates through the layered medium, we should consider two distinct situations: (a) the propagation occurs inside a homogeneous layer and (b) transmission occurs across an interface.

Figure 3 depicts a ray that traverses the homogeneous j-th layer (of velocity v_j) being transmitted (refracted) at the interface $j+1$. Let us denote by $R_{T,j}$ the wavefront radius of curvature at the initial point of the ray (that is, just below the j-th interface). The wavefront radius of curvature, $R_{I,j+1}$, just before transmission, satisfies the relationship

$$R_{I,j+1} = R_{T,j} + v_j \, \Delta t_j \ , \tag{1}$$

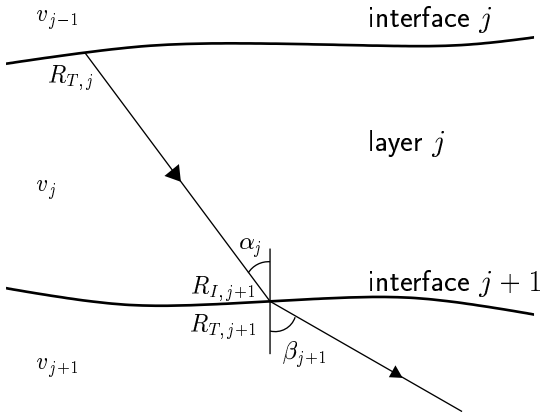

Figure 3: Ray propagation through layer j.

where Δt_j is the traveltime of the ray inside the layer. We now consider the change in wavefront curvature due to transmission at the interface. As shown in, e.g., Hubral

and Krey, 1980, we have

$$\frac{1}{R_{T,j+1}} = \frac{v_{j+1}\cos^2\alpha_j}{v_j\cos^2\beta_{j+1}}\frac{1}{R_{I,\,j+1}} + \frac{1}{\cos^2\beta_{j+1}}\left(\frac{v_{j+1}}{v_j}\cos\alpha_j - \cos\beta_{j+1}\right)\frac{1}{R_{F,\,j+1}}\,. \quad (2)$$

Here, α_j and β_{j+1} are the incident and transmission angles of the ray, respectively and $R_{F,j}$ is the interface radius of curvature, all these quantities being measured at the transmission point. Observe that Snell's law,

$$\frac{\sin\alpha_j}{v_j} = \frac{\sin\beta_{j+1}}{v_{j+1}}\,, \quad (3)$$

is valid. Assume now that the NIP is located at the $(N+1)$-th interface. This leads to the *focusing conditions*

$$R_{I,N+1} = 0 = R_{T,N} + v_N\,\Delta t_N \quad \text{and} \quad \Delta t_N = t_0 - \left(\sum_{j=1}^{N-1}\Delta t_j\right)\,, \quad (4)$$

that determine the velocity v_N. Here, $R_{I,N+1} = 0$ is the radius of curvature of the wavefront at the NIP (it starts as a point source) and $R_{T,N}$ is the radius of curvature of the wavefront after transmission across the interface N. Note that $R_{T,N}$, as given by setting $j = N-1$ in equation (2), has an implicit dependence on v_N and β_N. This is because

$$\sin\beta_N = \frac{\sin\alpha_{N-1}}{v_{N-1}}\,v_N\,, \quad (5)$$

by Snell's law. Once v_N and β_N are determined, the segment of the zero-offset ray inside the N-th layer can be constructed. The sought-for NIP location is then such that its distance to that transmission point is $v_N\Delta t_N$.

Summary of the Hubral and Krey algorithm

It is instructive to discuss the key ideas involved in the preceeding strategy. Firstly, we will present the main steps of the algorithm. Then, we will make some comments about the implementation of the various steps.

The method aims to extract a model composed by homogeneous layers separated by smoothly curved reflectors, corresponding to the well identified interfaces within the data only. This choice is made *a priori* by the user.

Determination of the first layer: The input data is, for each zero-offset ray, the traveltime t_0, the emergence angle β_0 and the wavefront curvature K_{NIP}. The velocity of the first layer is assumed to be known. Thus, only the reflector (the bottom of the first layer) should be determined. As explained below, this can be achieved in many different ways.

Determination of the jth-layer: Suppose that the model has been already determined up to the $(j-1)$th-layer. The method will proceed to the determination of the next layer, that is, the velocity of the jth-layer and the $(j+1)$th-interface. The input data is again, for each zero offset ray reflecting at the interface $(j+1)$, the traveltime t_0, the emergence angle β_0 and the wavefront curvature K_{NIP}. Trace the zero-offset ray down to the j-th interface. Recall that this ray makes the angle β_0 with the surface normal at its initial point. Now, using equations (1) and (2), back-propagate the NIP-wave from the surface to the j-th interface along that ray. Now use the focusing conditions (4) to determine the layer velocity v_j, the angle β_j and the NIP.

The above procedure can, in principle, be done to each zero-offset ray. However, under the constraint that the layer velocity v_j is constant, we obtain an over-determined system for that unknown. How to deal with this problem will be discussed below.

Brief discussion of the algorithm

We now discuss the above algorithm concerning its accuracy and implementation. Our aim is to identify those aspects that can be improved upon the introduction of the CRS methodology.

- The quantities needed by the method (emergence angles, normal traveltimes and NIP-wave radii of curvature) are not directly available, but have to be extracted from the data. In the description in Hubral and Krey, 1980, these quantities are obtained by conventional processing on CMP data.

- Note that the main idea of the method, the back-propagation of the NIP-wavefront, is carried out independently for each ray. Thus, in principle, each ray carries enough information to recover the layer velocity, that can be translated into many equations depending on the same unknown. Since we are assuming homogeneous layers, this implies an over-determination of the velocity. Of course, this question was faced on the original algorithm, but the methodology applied is not stated in the text. Hubral and Krey have pointed out that this "excess" of information could be used to improve the velocity distribution considered, for example, assuming a linear velocity variation.

- Note that the law of transmission for the wavefront curvatures depends on the curvature of the interface (R_F) at the transmission point, as we can see on formula (2). Hubral and Krey state that this can be obtained by a normal ray migration.

- As stated in Hubral and Krey, 1980, after the determination of the velocity, the location of each NIP can be obtained by down propagating the last ray segment. Since each ray hits the interface normaly, the local dip can also be determined.

In the next section we will show, with the help of the CRS attributes, that most of the difficulties addressed above can be solved. In this way, a more accurate and efficient version of the algorithm can be obtained and, moreover, preserving its elegant structure.

THE REVISED HUBRAL AND KREY ALGORITHM

In this section we discuss how to use the CRS parameters to fully supply the needs of the Hubral and Krey algorithm, and how to deal with the numerical aspects involved in. Then, we present a revised version of the original algorithm.

The obvious advantage of having the CRS parameters is that emergence angles and NIP-wavefront curvatures have been already determined. Thus, neither a velocity analysis nor a traveltime gradient estimation are required to obtain the input data for the inversion process. Moreover, with the help of the well-defined coherence section provided by the CRS method, it becomes easier to select the interesting horizon events.

The CRS method also provides the N-wavefront curvatures, that is not originally used by the Hubral and Krey algorithm. Recall that the N-wave associated to a zero-offset reflection is a wave that starts at the NIP, having the same curvature as the reflector. After the determination of a given interface, we can back-propagate the N-wavefront down to this interface, applying the same procedure we have described before for the back-propagation of the NIP-wavefront. Doing this, we have an approximation for the curvature of the reflector at the NIP that does not depend on how dense the NIPs are.

We have to take special care when dealing with estimated quantities as input data. We have to try to avoid or, at least, reduce the effect of the estimation errors on the inversion process. The strategy applied was to smooth the parameter curves. This makes physical meaning, since no abrupt variations on the parameters can in general occur. The method used is stated in Leite, 1998: To each five neighbors points on the curve, fits the least-square parabola and replace the middle point by its correspondent on the parabola (see Figure 4). This smoothing technique can be applied a fixed number of times (we use five) to each parameter curve.

The smoothing method described can be applied to any curve on the plane. All we need to know is how to follow the curve. In our case, the curves are parametrized by the central point coordinate. In caustic regions, many values of the parameter are associated to the same central point. This could generate a problem to find out the

Figure 4: For each five points, the smoothing scheme fits a parabola and replace the central point to its correspondent value on the parabola.

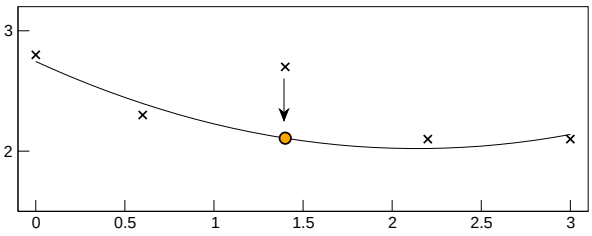

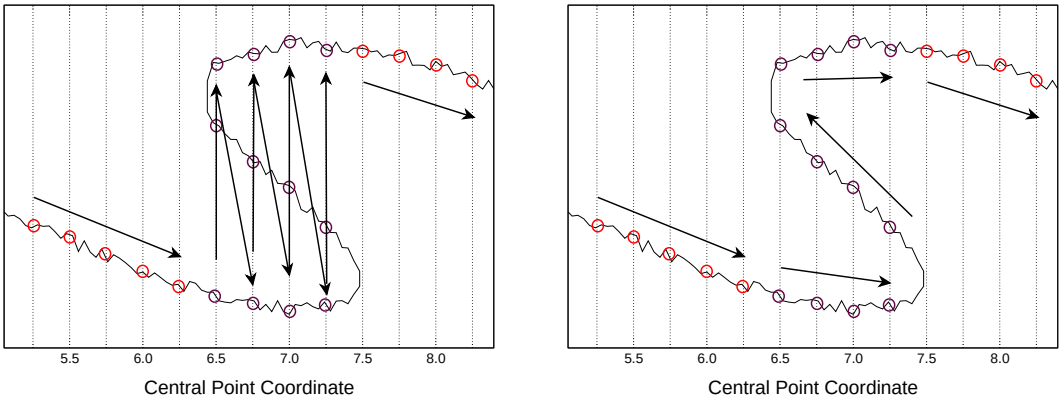

Figure 5: Both figures show a parameter curve within a caustic region. The small circles denote the sampled values of the parameter. At left, the points of the curve are sorted by their central point coordinates. The arrows indicate the sequence. At right, they were resorted to the correct sequence by the application of the unfolding criteria.

correct sequence. The reader could argue that perhaps the correct orders are already known. But, since the CRS parameters are extracted from the parameter sections by some picking process, the method we will describe could be used to automatically do this picking process. At the left side of Figure 5 we can see a situation where the parameters values are sorted by their central point coordinates.

We have formulated a criteria to unfold the parameter curve. When the curve has more than one value for the same central point coordinate, the proposed criteria tries to keep the variations of the CRS parameters between two neighbor points on the curve as small as possible. This is a reasonable assumption since a smooth behavior of the CRS parameters is expected. The merit function which is minimized is

$$F(\mathbf{p}_j, \mathbf{p}_i) = \frac{|t_0^j - t_0^i|}{t_0^i} + \frac{|\beta_0^j - \beta_0^i|}{|\beta_0^i|}\,, \tag{6}$$

where $\mathbf{p}_i = (x_0^i, t_0^i, \beta_0^i, K_{NIP}^i, K_N^i)$ denotes the vector of the CRS parameters, i is the index of the current point and j varies on the set of index of the neighbor point of the current point. We calculate the function above for each neighbor of point i and then the point that has obtained the minimum value is select to be next one in the reordered

sequence. We made tests including two more terms, one for K_{NIP} and one for K_N, but the stability of the method was reduced. Recall that this criteria should be applied before the smoothing process. So it must work even if there is noise in the parameters values. We have made several tests with this criteria and it really was able to unfold the curve.

We deal with the over-determination on the velocity considering a solution in the sense of least squares. By now, we are supposing a model with homogeneous layers, but this approach can be easily extended to incorporate velocity profiles depending for example, linearly on the depth.

Currently, we are recovering the interfaces by interpolating the many founded NIPs. Since this could lead to a not so smooth interface, what would be a disaster for the ray tracing process, we apply the same smoothing process described before to the interpolated interface. This really enhances the quality process overall.

Following, we present our implementation of the algorithm of Hubral and Krey, with the modifications discussed above.

Input data. Recall that after the application of the CRS method, we obtain a simulated zero-offset section in which the most important events (primary reflections) are well identified. This means that the traveltimes t_0 at each reflection is known. The identified primary reflections will provide the interfaces of the layered model to be inverted. Also recall that at each point of the zero-offset simulated section, we have attached the three parameters β_0, K_{NIP} and K_N extracted from the multi-coverage data. We shall make a consistent use of the CRS parameters along those identified reflections. We finally observe that the medium velocity in the vicinity of each central point is known a priori.

Determination of the first layer. For a given central point X_0, let t_0 be the zero-offset traveltime of the primary reflection from the first interface. Also, let β_0 be the emergence angle and K_N the radius of the N-wavefront curvature of the corresponding zero-offset ray. Draw from X_0 a straight line that makes an angle β_0 with the surface normal at X_0 and has length equals to $v_0 t_0/2$. The extreme of this segment of ray is the NIP. Do this for all central points that illuminate the first interface and then interpolate the inverted NIPs to recover the first interface. To minimize the noise on this first approximation, apply the smoothing process to the curve that describes the interface. We can now say that this first layer is completely determined. Before we go to the determination of the following layers, we will back-propagate all the N-waves associated to each ray. This provides an estimative of the curvature of the reflector at each NIP. Note that the curvature of the reflector will be necessary when we will back-propagate wavefront curvatures down to deeper layers, since to transpose the first interface we need to know its curvature.

Subsequent layers. As before, suppose that the model has been already determined up to the layer $(j-1)$. The input data is the CRS parameters for the zero-offset rays that reflect at the interface $(j+1)$. Trace the rays down to the interface j and back-propagate the NIP-wavefront along those rays. Applying the focusing conditions, estimate v_j by least squares. Using Snell's law calculate β_j and, knowing the remaining traveltimes, trace the last segment of each ray. Smooth the interpolated curve of the NIPs to obtain the interface $(j+1)$. Finally, along each zero-offset ray back-propagate the N-wavefront curvature to estimate the curvature of the interfaces.

SYNTHETIC EXAMPLE

The algorithm was applied to the model depicted on Figure 6, which consists of three interface separating four homogeneous layers. The second reflector has a synclinal region between 6.5km and 7.5km that generates caustics. For the three layers, we modeled the CRS parameters by using the dynamic ray tracing package Seis88, designed by Cervený and Psenck (see Cervený, 1985), and other auxiliar softwares developed by ourselves.

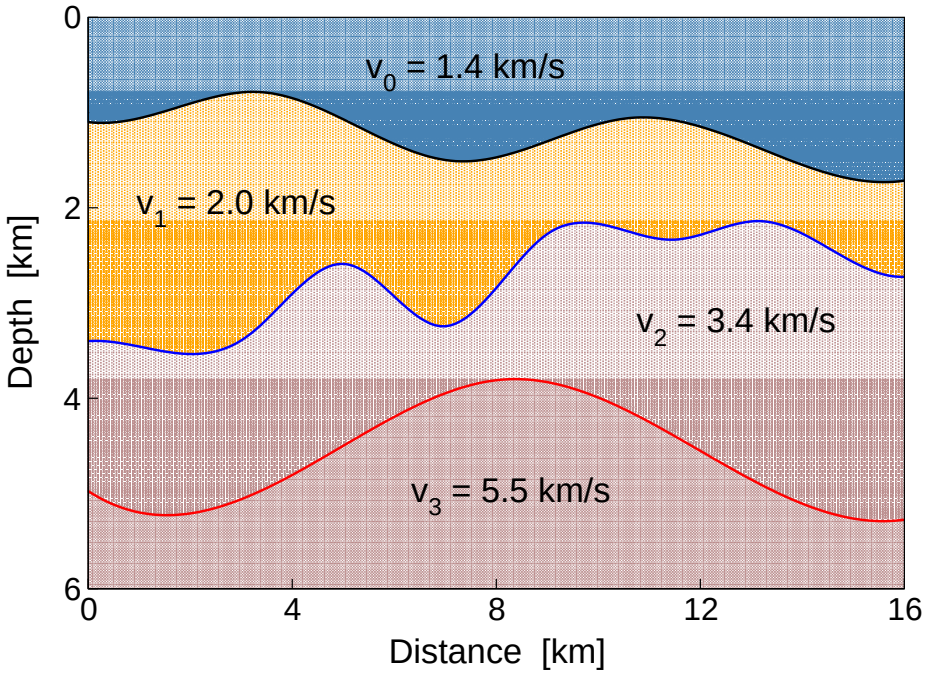

Figure 6: Synthetic model with four homogeneous layers.

As a validation test, we ran the method with the exact modeled parameters as the input data. As expected, the velocities and interfaces were recovered with the same

precision of the modeled input data.

The second and more realistic test were achieved with the CRS parameters with 10% of white noise on all parameters as the input data. We show in Figure 7 the inverted model. Note that the velocities were very well recovered, with relative errors of $1,31\%$ and $2,65\%$, for the second and third layers, respectively. But the third reflector still has outliers. This problems is due to a not so smooth interpolation of the recovered points of the second reflector. This problem damages the ray tracing process subsequently carried out for the deeper layers.

NEXT STEPS

We plan to make two major improvements. The first one concerns a better recovering of the interfaces. The idea is, once the NIPs were recovered, instead of interpolating them, fit a smooth curve, like a cubic spline, for example. In fact, we are plannig to do this with the parametric interpolating curve present in Hildebrand, 1990. The interpolating curve is a picewise cubic polynomial in the innner intervals and a parabola at the extreme intervals. This options is cheaper then cubic splines because, given the points to be interpolated, the interpolating curve can be computated directly, without solving linear systems. We believe that this modification will solve the problem seen on the estimation of the third reflector of the presented example (Figure 7).

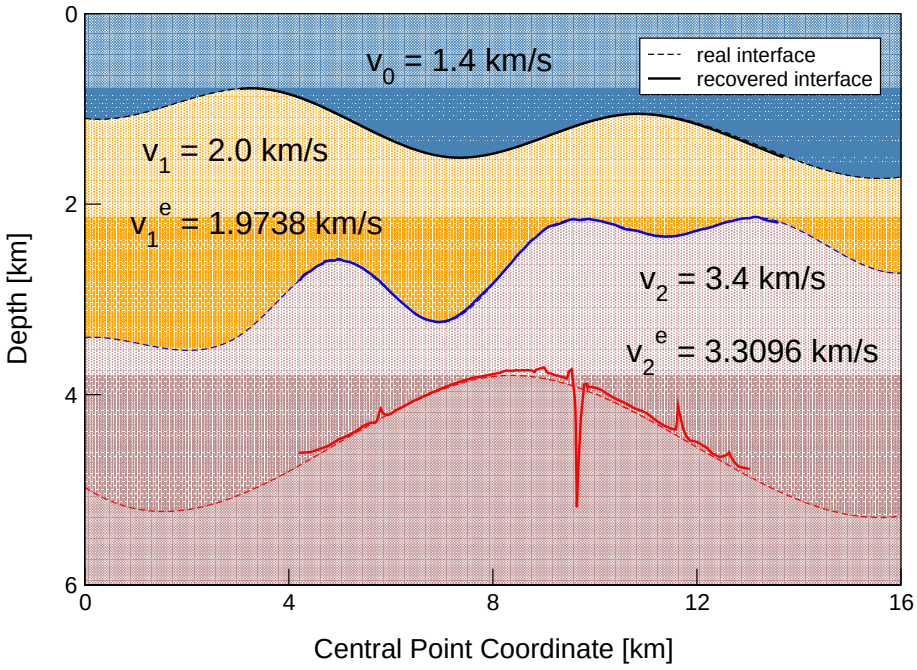

Figure 7: Inverted model. v_j and v_j^e are the real and estimated velocities, respectively. The solid curves are the inverted interfaces.

We also plan to modify the software so that the estimated velocity could linearly variate with the depth. This implies only on a minor modification on the estimation of the layer velocities and on the ray tracing method.

CONCLUSIONS

The contribuion of this work is a new implementation of the Hubral and Krey algorithm, using the CRS parameters. We also discuss details of the numerical implementation of the algorithm, needed for a efficient application of the method.

The results are encouraging. We strongly believe that the method will be available for use as soon as the implementation of the approximation of the interfaces by smooth curve will be finished.

Concerning more complex velocity profiles, we could run the algorithm for separeted parts of the domain. Thus, each inverted model would be composed by homogeneous layers that could be glued to form a complete inverted model, homogeneous by parts. This approach can be adopted independently of the inclusion of the possibility of velocity profiles depending on the depth.

REFERENCES

Berkhout, A., 1984, Seismic resolution, a quantitative analysis of resolving power of acoustical echo techniques: Geophysical Press.

Beylkin, G., 1985, Imaging of discontinuities in the inverse scattering problem by inversion of a generalized Radon transform: J. Math. Phys., **26**, no. 1, 99–108.

Birgin, E. G., Biloti, R., Tygel, M., and Santos, L. T., 1999, Restricted optimization: a clue to a fast and accurate implementation of the Common Reflection Surface stack method: Journal of Applied Geophysics, **42**, no. 3–4, 143–155.

Bleistein, N., 1984, Mathematical methods for wave phenomena: Academic Press, New York.

Bleistein, N., 1987, On the imaging of reflectors in the earth: Geophysics, **52**, no. 7, 931–942.

Bojarski, N., 1982, A survey of the near-field far-field inverse scattering inverse source integral equation: IEEE Trans. Ant. Prop., **AP-30**, no. 5, 975–979.

Cervený, V., 1985, Ray synthetic seismograms for complex two-dimensional and three-dimensional structures: J. Geophys., **58**, 44–72.

Cohen, J., Hagin, F., and Bleistein, N., 1986, Three-dimensional Born inversion with an arbitrary reference: Geophysics, **51**, no. 8, 1552–1558.

Hildebrand, W., 1990, Connecting the Dots Parametrically: An Alternative to Cubic Splines: The College Mathematics Journal, **21**, no. 3, 208–215.

Hubral, P., and Krey, T., 1980, Interval velocities from seismic reflection traveltime measurements: Soc. Expl. Geophys.

Hubral, P., Schleicher, J., and Tygel, M., 1992, Three-dimensional paraxial ray properties – Part I. Basic relations: J. Seism. Expl., **1**, no. 3, 265–279.

Hubral, P., 1983, Computing true amplitude reflections in a laterally inhomogeneous earth: Geophysics, **48**, no. 8, 1051–1062.

Langenberg, K., 1986, Applied inverse problems for acoustic, electromagnetic, and elastic wave scattering *in* Sabatier, P., Ed., Basic methods in Tomography and Inverse Problems:: Adam Hilger.

Leite, L., 1998, Introduçao a análise espectral em geofisica: FADESP, Belém, Brasil.

Martins, J., Schleicher, J., Tygel, M., and Santos, L., 1997, 2.5-d true-amplitude Kirchhoff migration and demigration: J. Seism. Expl., **6**, no. 2/3, 159–180.

Porter, R., 1970, Diffraction-limited scalar image formation with holograms of arbitrary shape: J. Acoust. Soc. Am., **60**, no. 8, 1051–1059.

Ricker, N., 1953, The form and laws of propagation of seismic wavelets: Geophysics, **18**, no. 01, 10–40.

Rockwell, D., 1971, Migration stack aids interpretation: Oil and Gas Journal, **69**, 202–218.

Schleicher, J., Hubral, P., Tygel, M., and Jaya, M., 1997, Minimum apertures and Fresnel zones in migration and demigration: Geophysics, **62**, no. 2, 183–194.

Schneider, W., 1978, Integral formulation for migration in two and three dimensions: Geophysics, **43**, no. 1, 49–76.

Sommerfeld, A., 1964, Optics:, volume IV of **Lectures on Theoretical Physics** Academic Press, New York.

Tygel, M., Schleicher, J., and Hubral, P., 1994, Pulse distortion in depth migration: Geophysics, **59**, no. 10, 1561–1569.

Tygel, M., Schleicher, J., and Hubral, P., 1995, Dualities between reflectors and reflection-time surfaces: J. Seis. Expl., **4**, no. 2, 123–150.

Tygel, M., Müller, T., Hubral, P., and Schleicher, J., 1997, Eigenwave based multiparameter traveltime expansions: Eigenwave based multiparameter traveltime expansions:, 67th Annual Internat. Mtg., Soc. Expl. Geophys., Expanded Abstracts, 1770–1773.

Tygel, M., Schleicher, J., Santos, L., and Hubral, P., 2000, An asymptotic inverse to the Kirchhoff-Helmholtz integral: Inv. Probl., **16**, 425–445.

Vermeer, G., 1999, Factors affection spatial resolution: Geophysics, **64**, no. 3, 942–953.